Prospects of constraining magnetic fields using their effects on CMB, LSS and ionisation history

Kerstin Kunze

(University of Salamanca and IUFFyM)

KK   PRD 83 (2011) 023006; PRD 85 (2012) 083004; PRD 87 (2013) 103005; PRD 89 (2014) 103016
KK, E. Komatsu, JCAP 1506 (2015) 06, 027
KK, E. Komatsu, JCAP 1401 (2014) 01, 009

Cosmological magnetic fields present since before decoupling affect the cosmic microwave background (CMB):

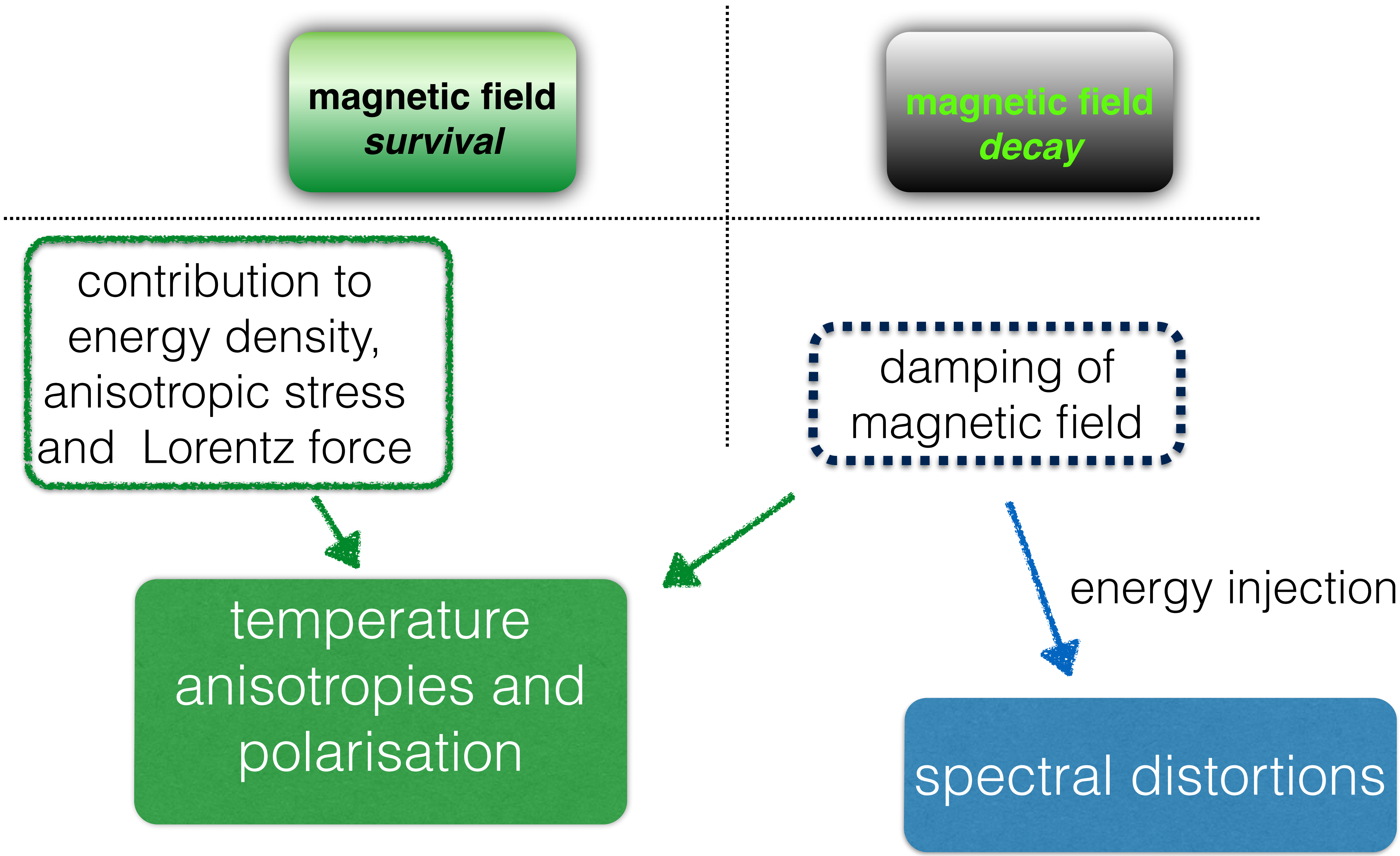

CMB anisotropies and polarisation induced by **contribution** of *stochastic* helical magnetic field

$$\langle B_i^*(\vec{k})B_j(\vec{q})\rangle = \delta_{\vec{k},\vec{q}}\mathcal{P}_S(k)\left(\delta_{ij} - \frac{k_i k_j}{k^2}\right) + \delta_{\vec{k}\vec{k}'}P_A(k)i\epsilon_{ijm}\hat{k}_m$$

amplitude

upper cut-off

damping scale

where

$$\mathcal{P}_M(k, k_m, k_L) = A_M\left(\frac{k}{k_L}\right)^{n_M} W(k, k_m)$$

$$M = S, A$$

window function

pivot scale

$$W(k, k_m) = \pi^{-\frac{3}{2}} k_m^{-3} e^{-(k/k_m)^2}$$

- **Primary** CMB anisotropies and polarisation induced by **contribution** of *helical* magnetic field

distinctive signature of helical magnetic field

ANGULAR POWER SPECTRA FOR SCALAR,VECTOR AND TENSOR MODES

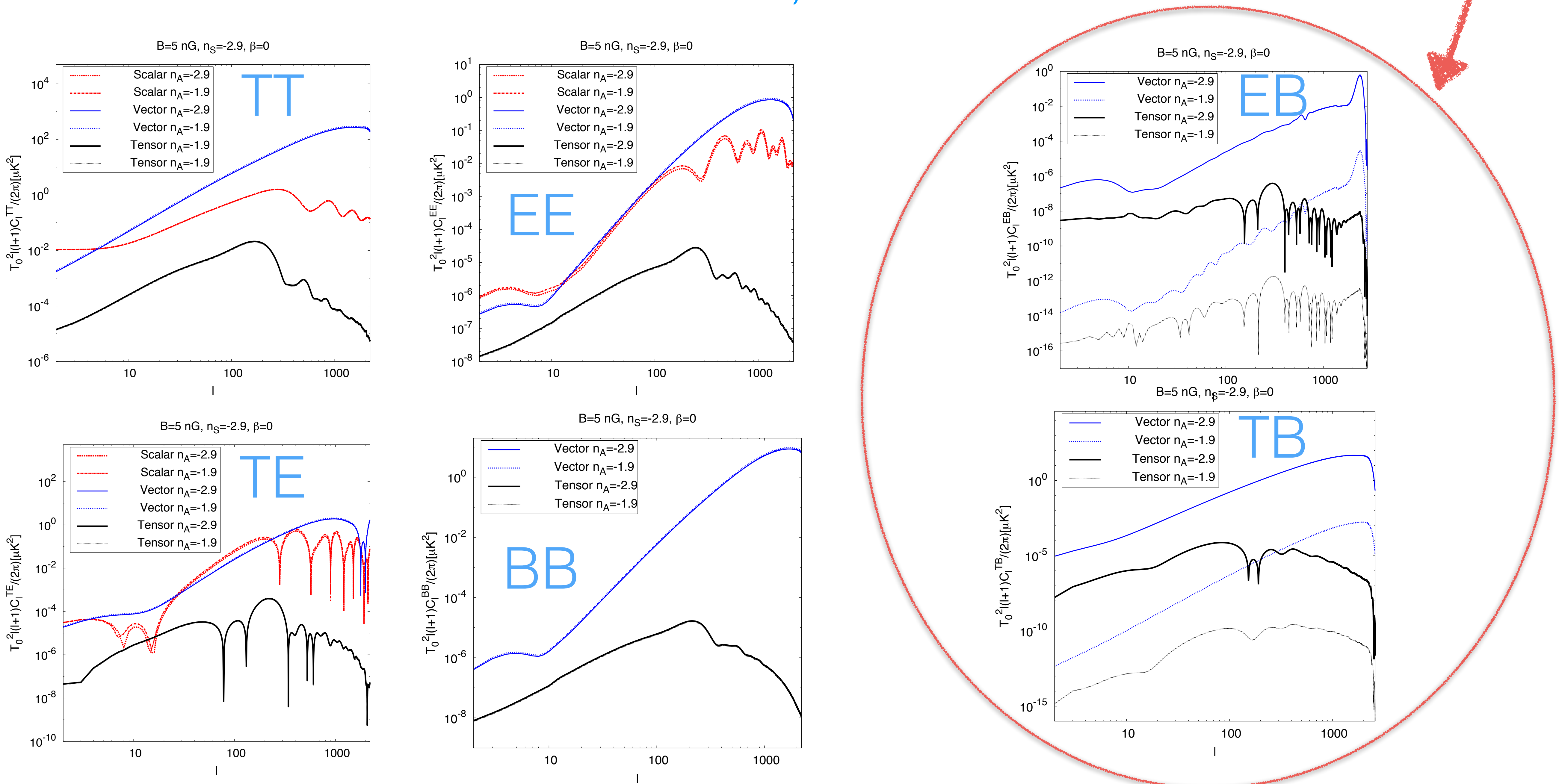

KK ‘12

MODIFIED VERSION OF CMBEASY

- Bulk motions of electrons along the line of sight induce **secondary** temperature fluctuations in the postdecoupling, reionized universe.

$$\Theta(\hat{\boldsymbol{n}}) = \int dDg(D)\hat{\boldsymbol{n}} \cdot \boldsymbol{V}_b(\boldsymbol{x}),$$

Fluctuations in baryon energy density along line-of-sight change number density of potential scatterers for CMB photons, thus change scattering probability and visibility function.

$$\delta \boldsymbol{V}_b(\boldsymbol{x}, \eta) = \Delta_b(\boldsymbol{x}, \eta)\boldsymbol{V}_b(\boldsymbol{x}, \eta).$$

- In the presence of a magnetic field not only the scalar mode but also the vector mode source bulk motions.

KK ‘14

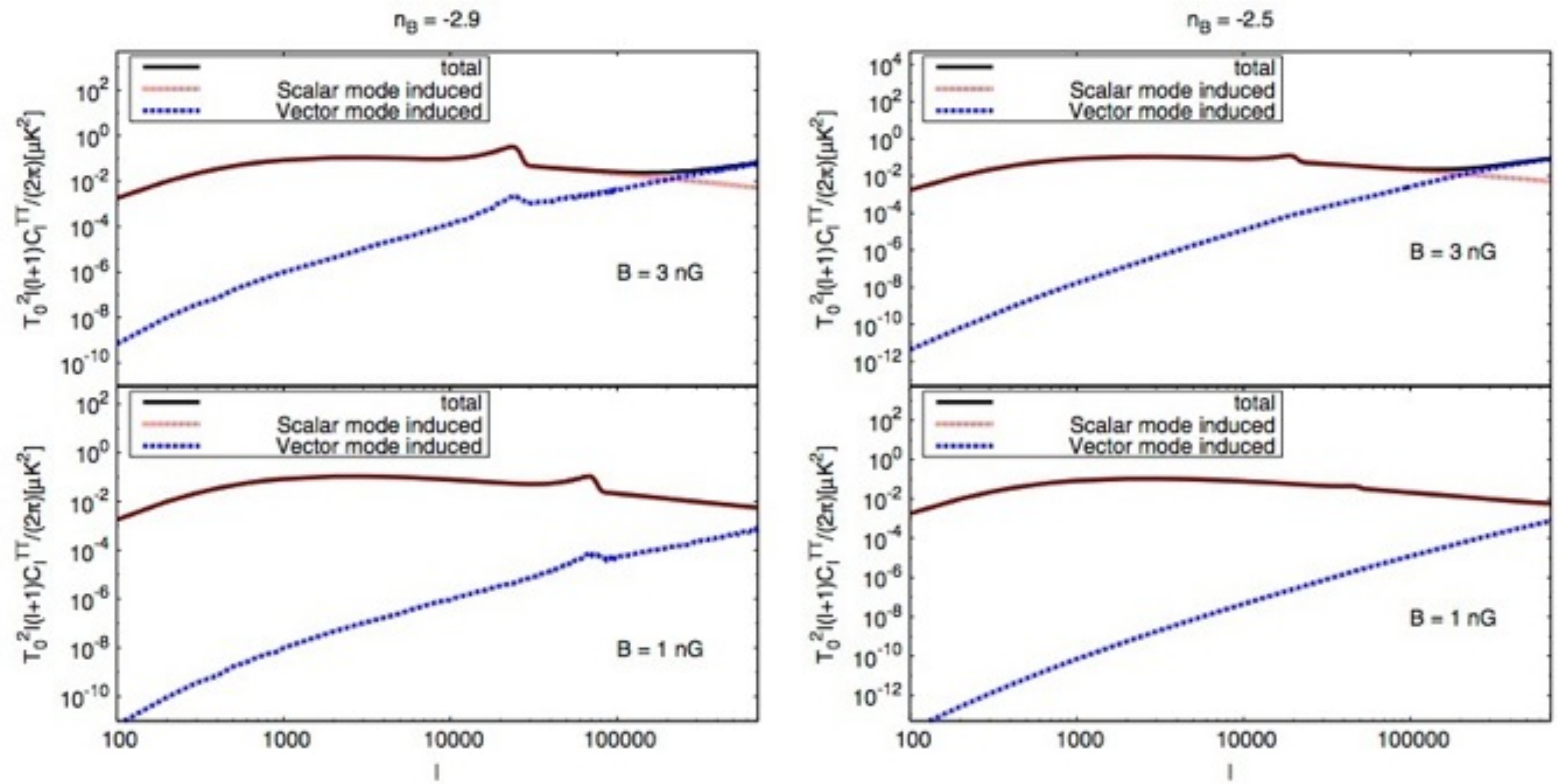

Induced **secondary** temperature anisotropies

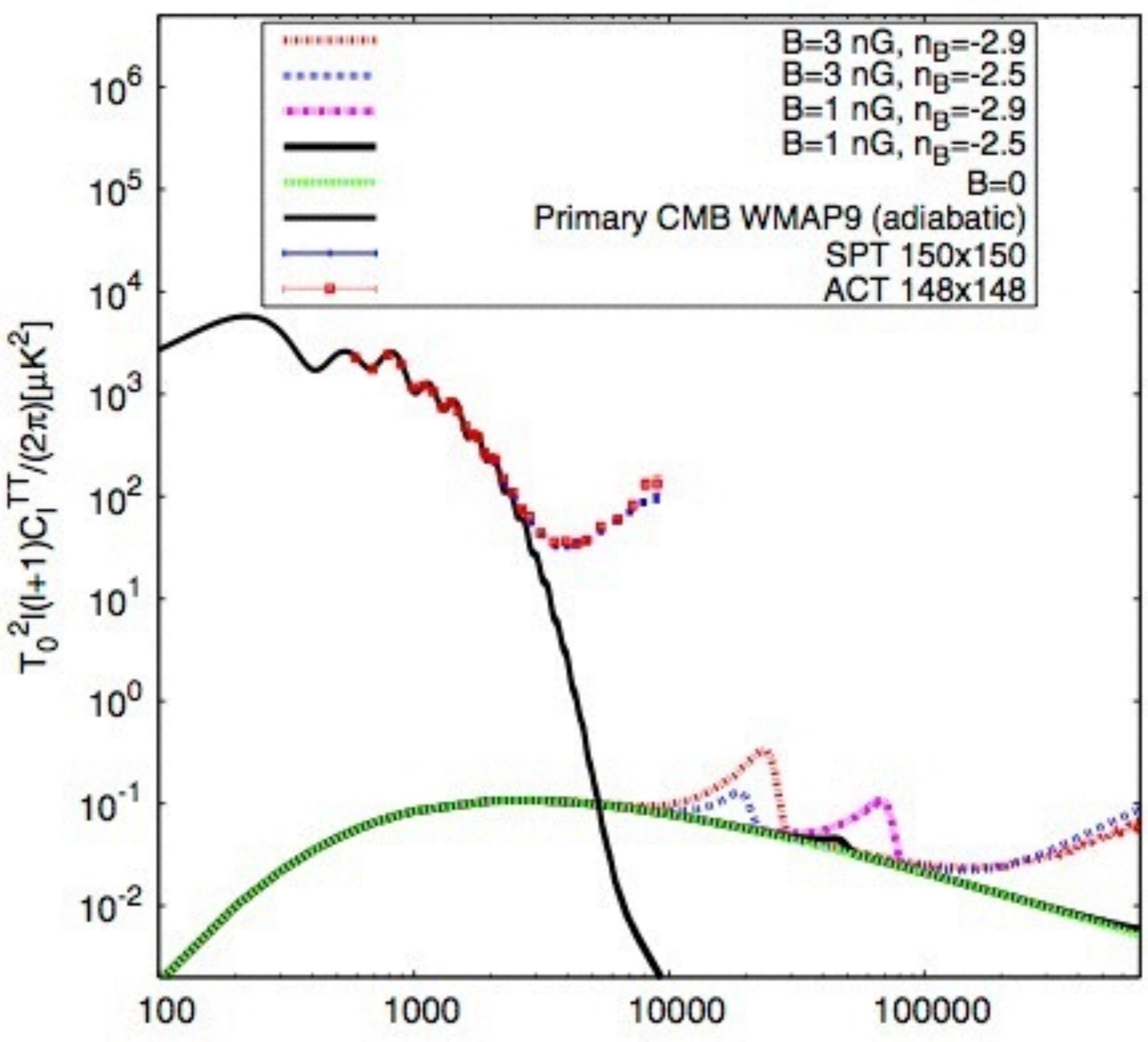

KK ‘14

Future observations with ALMA might reach

$$10^4 < \ell < 10^6$$

Atacama Large Millimeter/submillimeter Array (ALMA): ALMA - the largest astronomical project in existence- is a single telescope of revolutionary design, composed of 66 high precision antennas located on the Chajnantor plateau, 5000 meters altitude in northern Chile.

Linear matter power spectrum

total matter perturbation

$$\Delta_m \equiv R_c \Delta_c + R_b \Delta_b$$

$$R_i \equiv \frac{\rho_i}{\rho_{matter}}$$

(during matter domination)

$$\ddot{\Delta}_m + \mathcal{H}\dot{\Delta}_m - \frac{3}{2}\mathcal{H}^2\Delta_m = \mathcal{H}^2\Omega_\gamma\Delta_B - \frac{k^2}{3}\Omega_\gamma L$$

on very small scales

$$\Delta_m \propto k^2 L$$

$$\Rightarrow \mathcal{P}_{\Delta_m} \propto k^4 \mathcal{P}_L$$

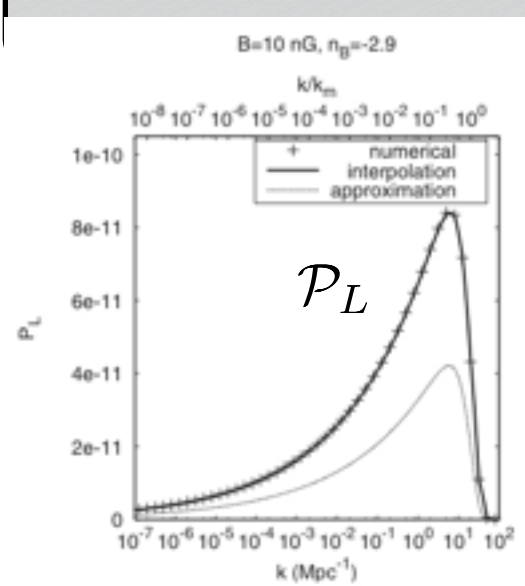

Shaw, Lewis '10

total linear matter power spectrum due to:

the compensated magnetic mode

standard adiabatic mode plus compensated magnetic mode assuming they are uncorrelated

KK '11

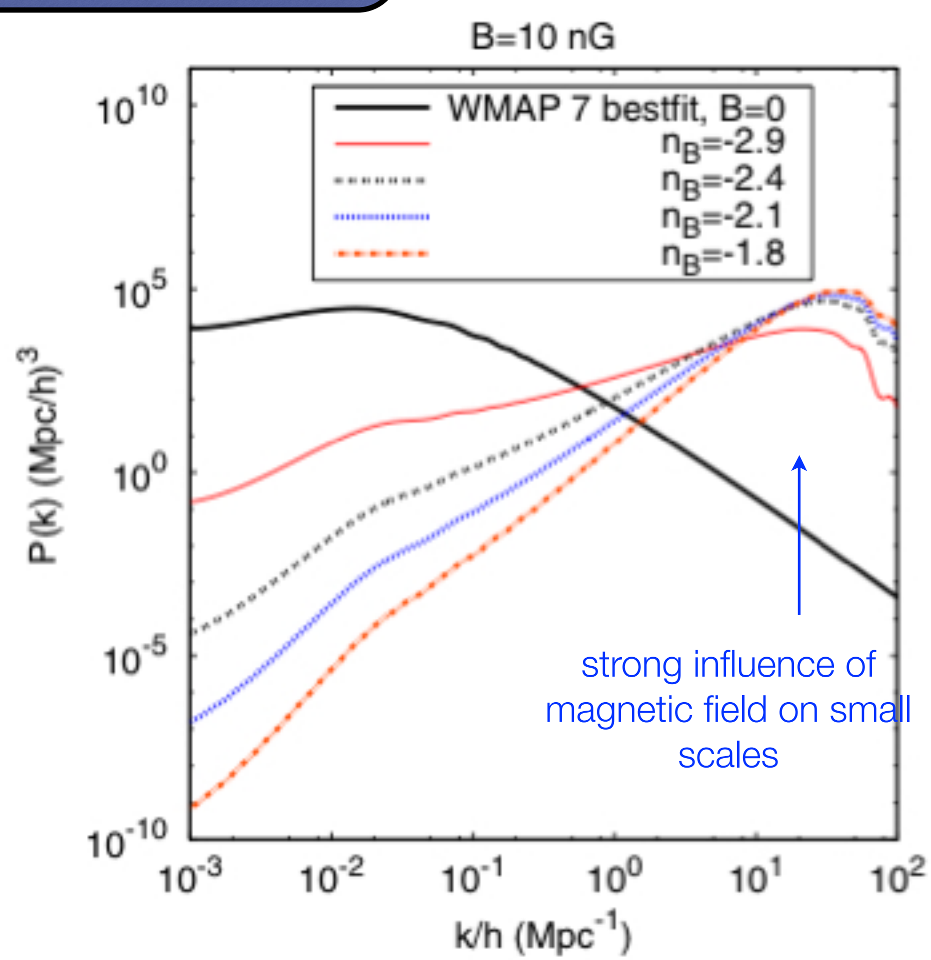

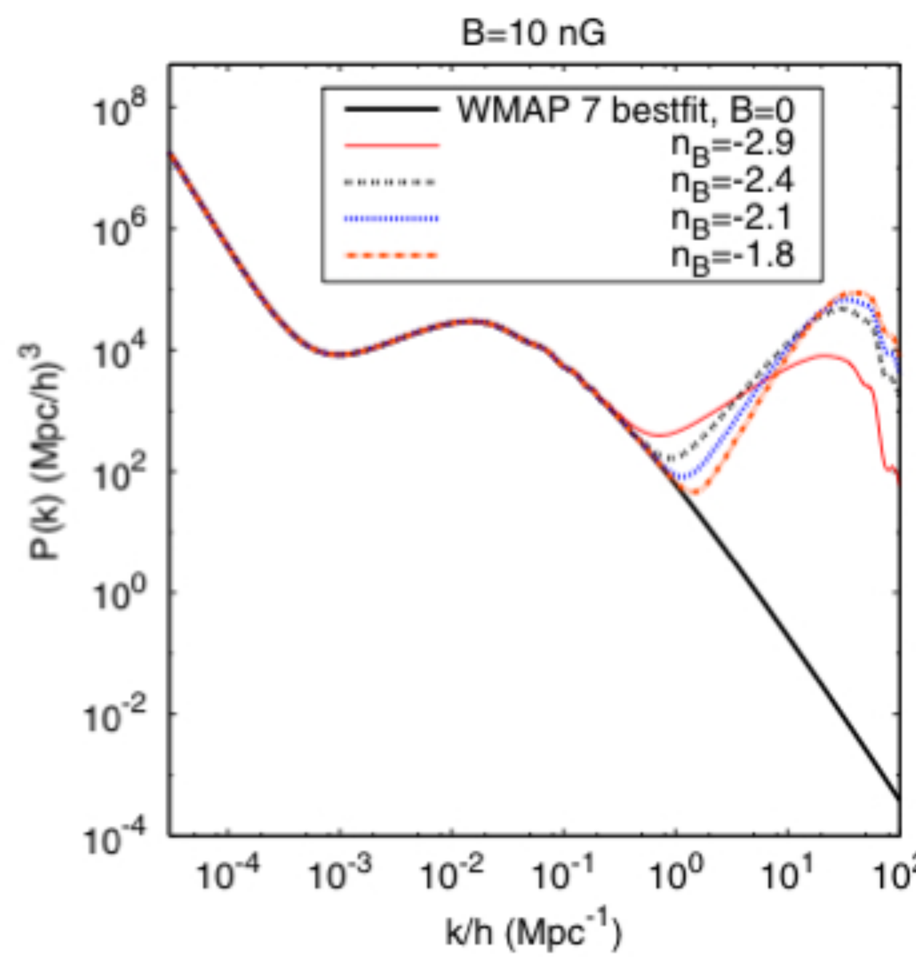

Other interesting aspects to test:

Cross correlations between adiabatic and magnetic modes: testing the generation mechanism

- generation of magnetic field during inflation: coupling electrodynamics to scalar field.

$$S = \int d^4x\sqrt{-g}\left(-\frac{1}{4}W(\phi)F_{\mu\nu}F^{\mu\nu} - \frac{1}{2}(\partial\phi)^2 - V(\phi)\right)$$

- 3-point function (Caldwell et al . (2011)):

$$\langle \delta\phi B_i B_j\rangle \Rightarrow \langle \zeta\Delta_B\rangle,\ \langle\zeta\pi_B\rangle$$

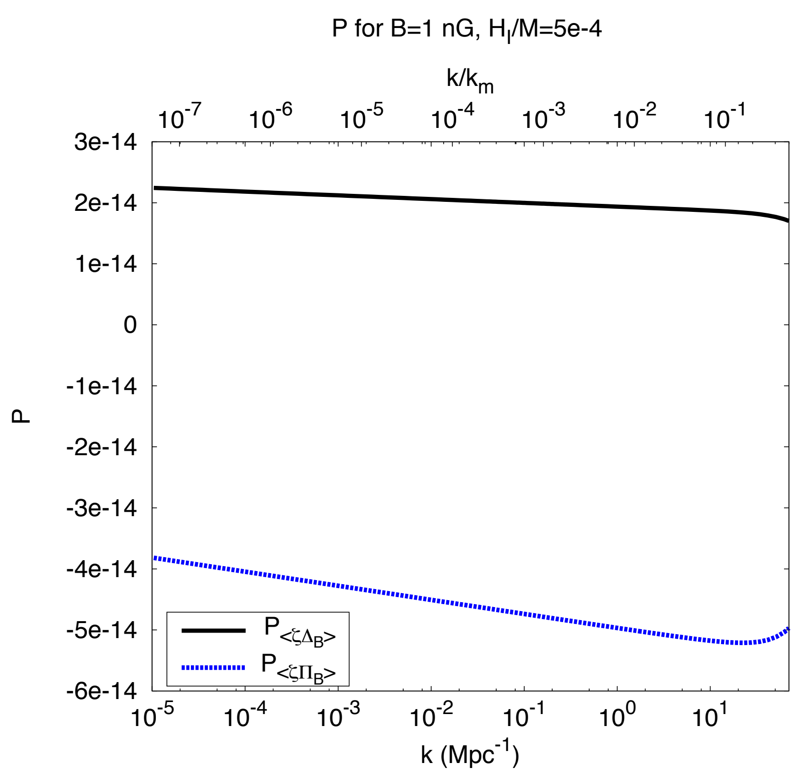

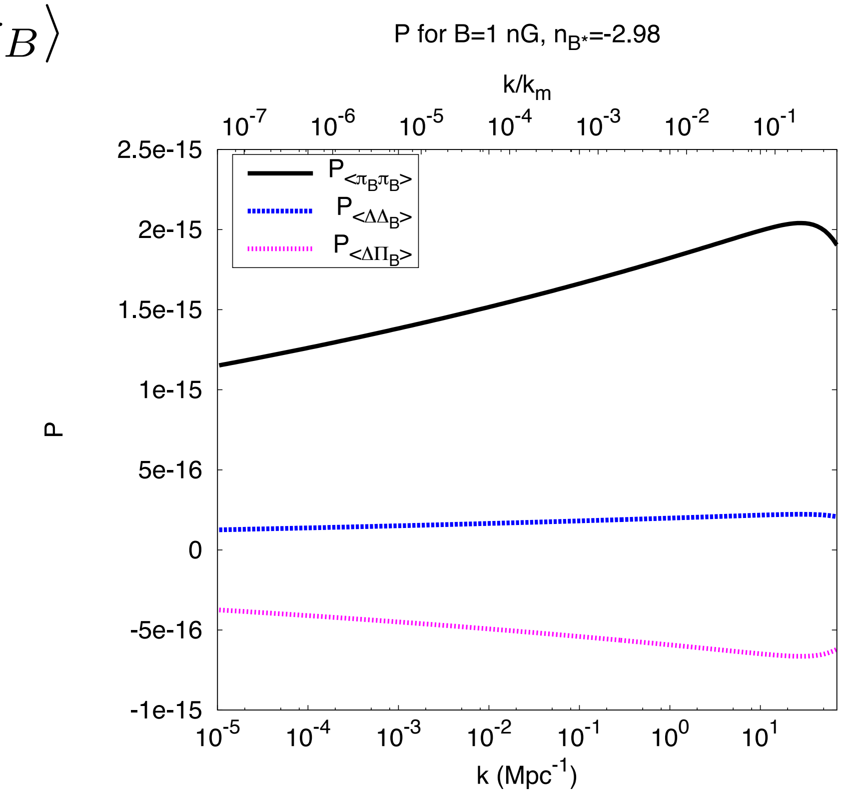

Cross correlations between adiabatic and magnetic modes

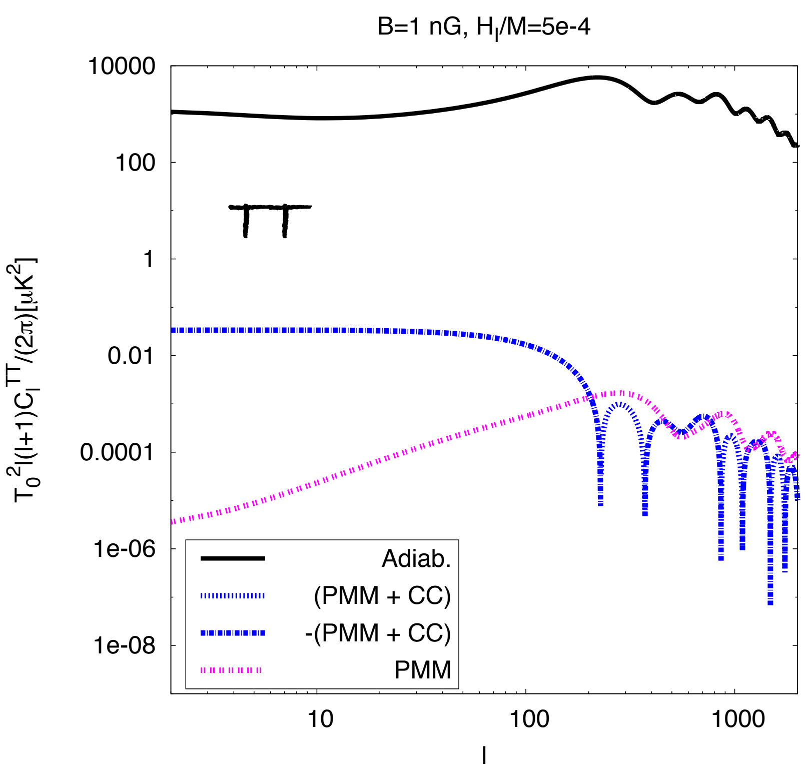

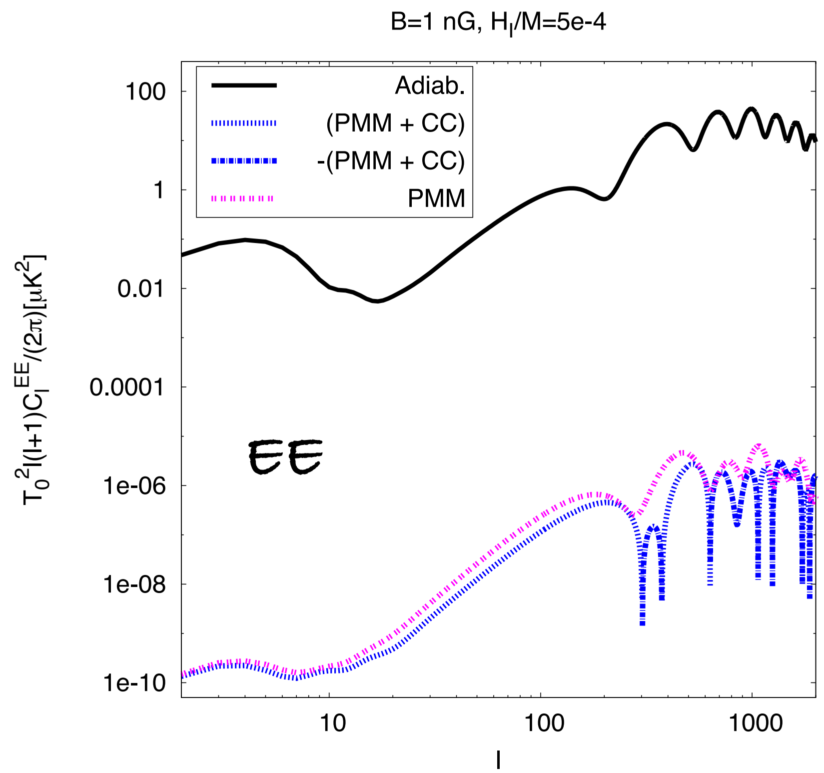

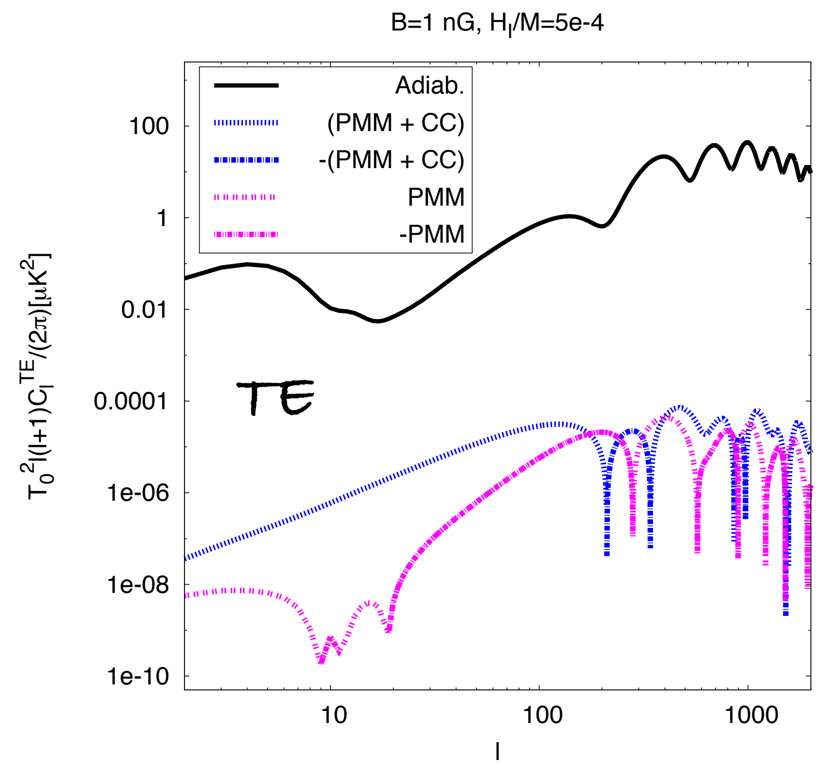

LINEAR MATTER POWER SPECTRUM

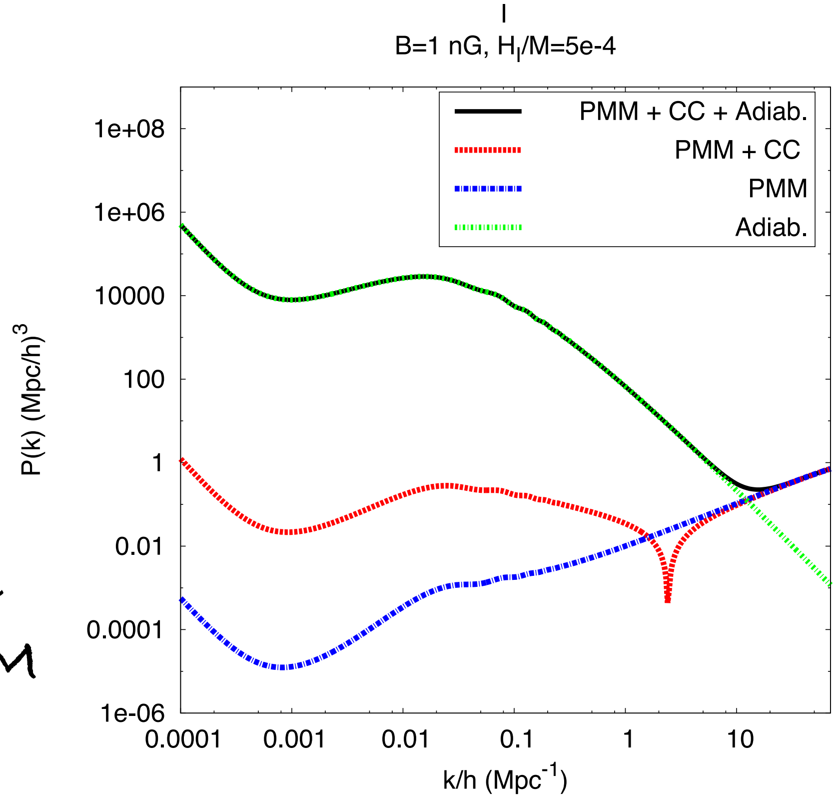

B=1 NG, S.I.

KK '13

Damping of magnetic fields

There is also damping around neutrino decoupling at around z~ 10^{10} when a black body spectrum is always restored.

- Before decoupling of photons
  - ★ viscous damping
- After decoupling of photons
  - ★ decaying MHD turbulence
  - ★ ambipolar diffusion

*Damping in the **pre-decoupling** era*

Subramanian, Barrow 1998
(nonlinear treatment)

In a magnetized plasma: 3 additional modes

Jedamzik, Katalinic, Olinto 1998

- Fast magnetosonic modes: damp similarly to sonic waves (Silk damping)

damping wave number $k_d = k_\gamma$

inverse of usual photon diffusion scale

- Slow magnetosonic and Alfvén modes: overdamped limit

damping wave number $k_d = \dfrac{k_\gamma}{v_A \cos\theta}$

angle between background field direction and wave vector

Alfvén velocity $v_A \sim B_0/\sqrt{\rho + p}$

$$v_A = 3.8 \times 10^{-4} \left(\frac{B_0}{1\mathrm{nG}} \right)$$

*Damping in the **post-decoupling** era*

Ambipolar diffusion

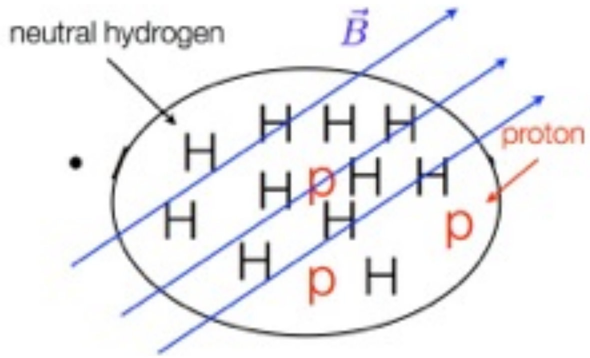

Lorentz force only acts on ionized component

↓

$$\vec{v}_{ion} \neq \vec{v}_{neutral}$$

↓

Resisting the relative drift is a frictional (drag) force due to mutual collisions between ions and neutrals.

↓

Heating of IGM and dissipation of magnetic energy

After decoupling radiative viscosity dramatically drops. However magnetic fields can still be damped.

Decaying MHD turbulence

After decoupling turbulence no longer suppressed, nonlinear interactions transfer energy to smaller scales, dissipating magnetic field on large scale, inducing MHD turbulence to decay.

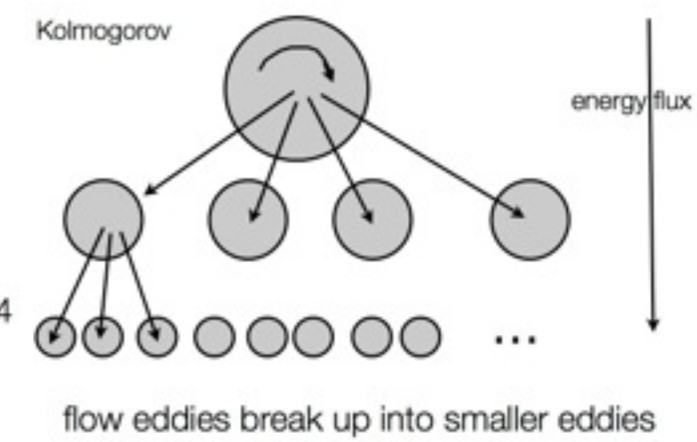

non helical

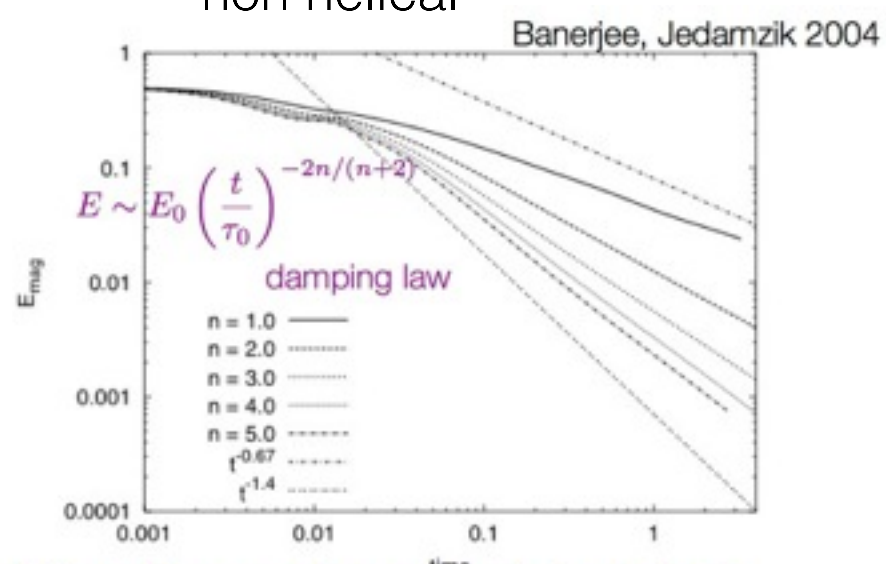

Evolution of magnetic energy in turbulent regime for different initial energy spectra n. $(E_k \sim k^n)$

(inverse cascade also for non helical fields: Kahniashvili et al. '13, '14, '15)

Kahniashvili et al.

PHYSICAL REVIEW D **87,** 083007 (2013)

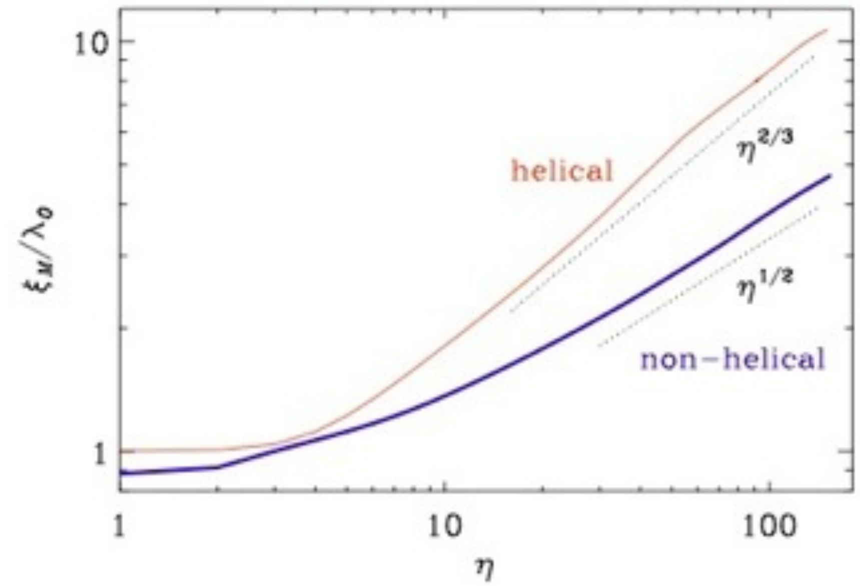

FIG. 1 (color online). $\xi_M(\xi)$ for helical (thin, red) and non-helical (thick, blue) cases.

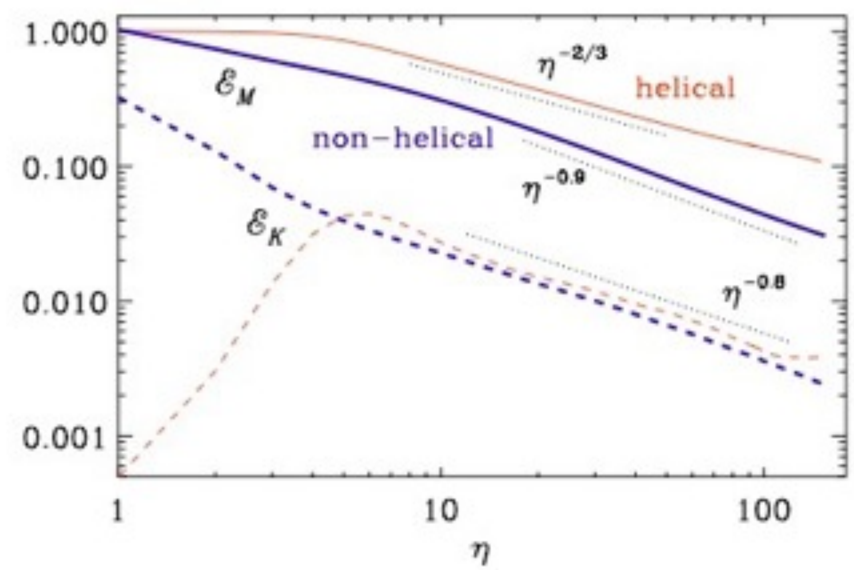

FIG. 2 (color online). $\mathcal{E}_M(\xi)$ (solid) and $\mathcal{E}_K(\xi)$ (dashed) for the helical (thin, red) and nonhelical (thick, blue) cases.

Ambipolar diffusion

Decaying MHD turbulence

Evolution of electron temperature (Sethi, Subramanian '05)

$$\dot{T}_e = -2\frac{\dot{a}}{a}T_e + \frac{x_e}{1+x_e}\frac{8\rho_\gamma\sigma_T}{3m_e c}(T_\gamma - T_e) + \frac{x_e\Gamma}{1.5k_B n_e}$$

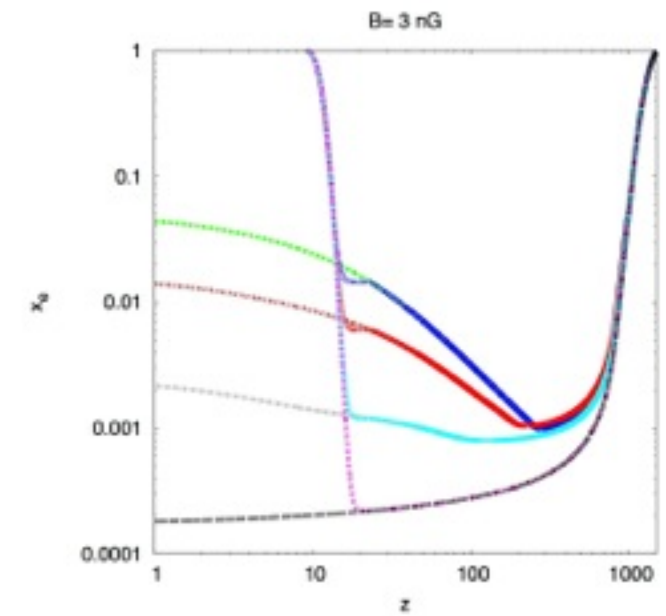

$$\Gamma = \Gamma_{\rm in} + \Gamma_{\rm decay}$$

$$\Gamma_{\rm in} \propto (1+z)^{3.625}(1-x_e)/x_e$$

$$\Gamma_{\rm decay} \propto (1+z)^{5.5}$$

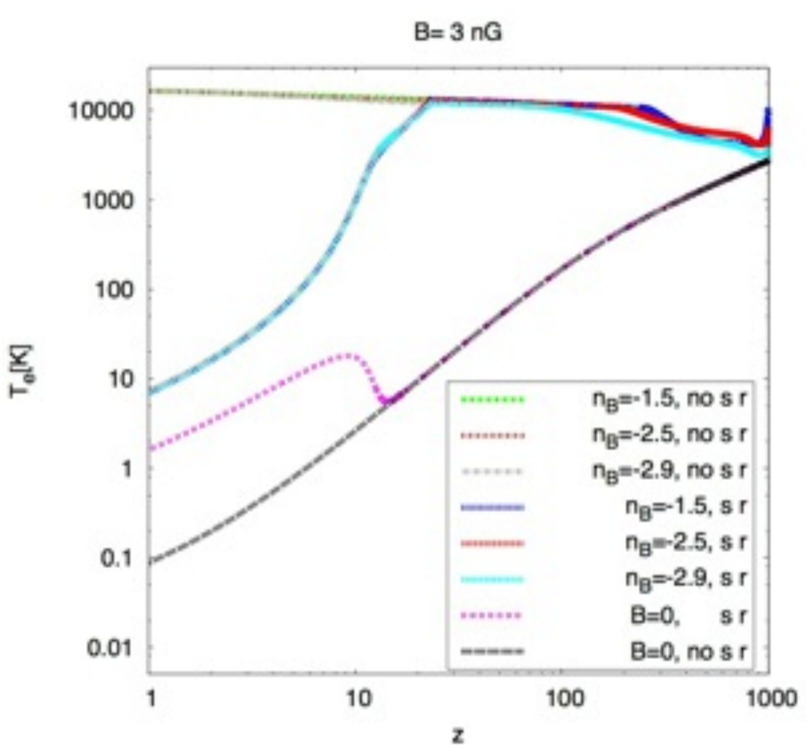

important at late times

$z < 100$

important at early times

$z > 100$

KK, Komatsu '15

CMB spectral distortions

- Spectrum well fitted by Planck black body spectrum

$$n_\nu = \left[\exp\left(\frac{h\nu}{kT}\right) - 1\right]^{-1}$$

$$B_\nu(T) = \frac{2h\nu^3/c^2}{\exp\left(\frac{h\nu}{kT}\right) - 1}$$

FIXSEN ET AL. 1996

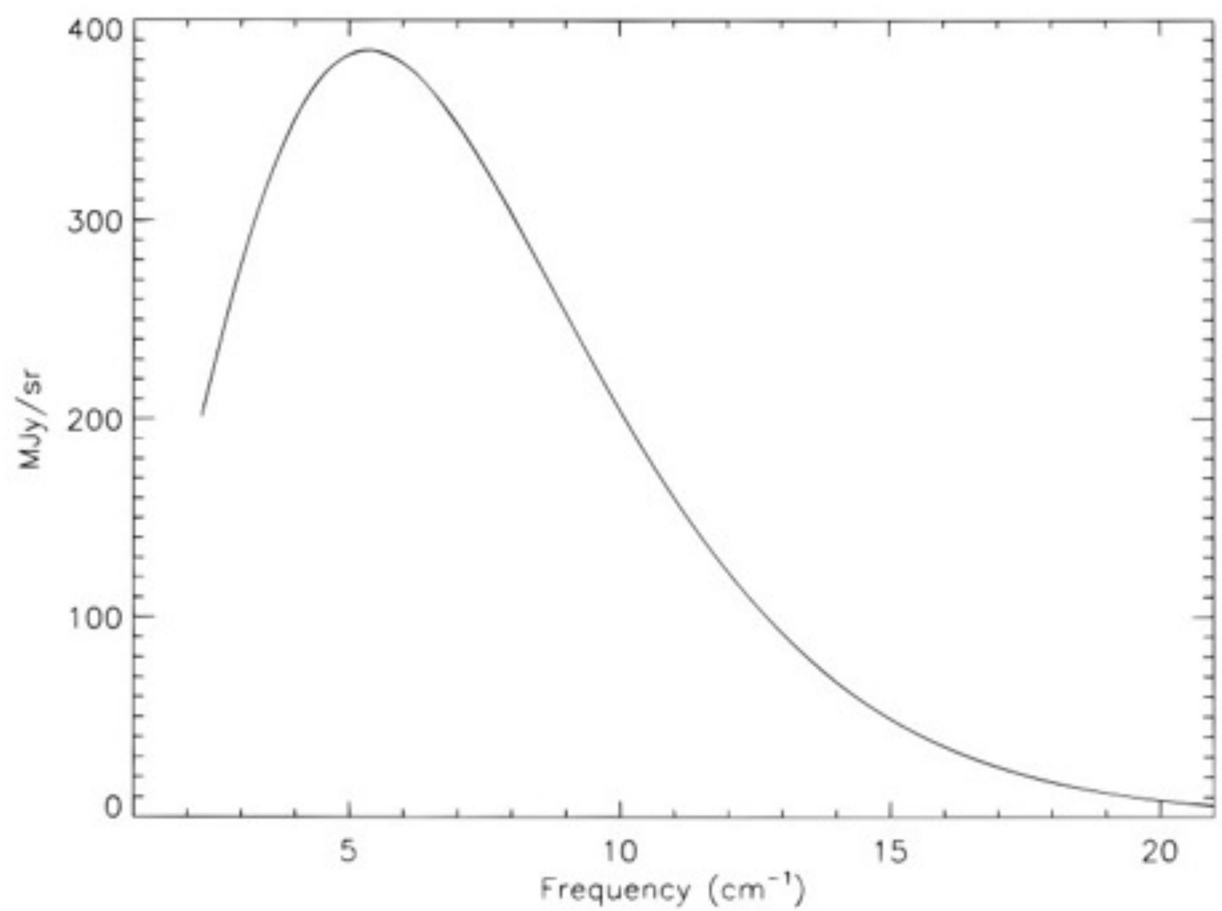

FIG. 4.—Uniform spectrum and fit to Planck blackbody (T). Uncertainties are a small fraction of the line thickness.

- Spectral distortions: y- and μ-type are small

Origin of CMB spectral distortions

Energy injection

due to:

- $m\bar{m} \to \gamma\gamma$
  $X \to ...\gamma$
- damping of small scale density perturbations before recombination
- .....
- damping of magnetic fields: before and after recombination

at some redshift z_{inj}

thermal background radiation

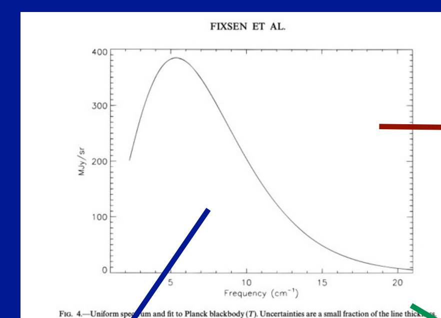

$z_{inj} < 5 \times 10^4$

elastic Compton scattering becomes ineffective

$\downarrow$

$$B_\nu(T) + y\frac{\partial S_y}{\partial y} \qquad y = \int \frac{k(T_e - T_\gamma)}{m_e c^2} d\tau_e$$

y-type distortion

$z_{inj} > 2 \times 10^6$

bremsstrahlung

$$e^- + X \to e^- + X + \gamma$$

double (inelastic) Compton scattering

$$e^- + \gamma \to e^- + \gamma + \gamma$$

$\downarrow$

Planck spectrum

$5 \times 10^4 < z_{inj} < 2 \times 10^6$

elastic Compton scattering

$$e^- + \gamma \to e^- + \gamma$$

$\downarrow$

Bose-Einstein spectrum

$$f = [\exp(\mu + h\nu/kT_e) - 1]^{-1}$$

μ-type distortion

Hu, Silk 1993

Sunyaev, Zeldovich 1970
Illarionov, Sunyaev 1975
Burigana, Danese, DeZotti 1991
Hu, Scott, Silk 1994
Jedamzik, Katalinic, Olinto 2000
Khatri, Sunyaev, Chluba 2012
Khatri, Sunyaev 2012

time scale for double Compton scattering

$$t_{DC} = 2.06\times 10^{33}\left(1-\frac{Y_P}{2}\right)^{-1}(\Omega_b h^2)^{-1} z^{-\frac{9}{2}}\ \mathrm{s}$$

Hu, Silk 1993

Pre-decoupling era

μ-type distortion

$$\frac{d\mu}{dt} = -\frac{\mu}{t_{DC}(z)} + \frac{1.4}{3}\frac{\frac{dQ}{dt}}{\rho_\gamma}$$

mixture of black body spectra: 1/3 of injected energy leads to spectral distortions, 2/3 to raise average temperature (Khatri, Sunyaev, Chluba 2012)

constraints

COBE/FIRAS		$B_0 < 0.4\ \mathrm{nG}$	$n_B = -2.2$
$\lvert\mu\rvert < 9\times 10^{-5}$	$\Rightarrow$	$B_0 < 40\ \mathrm{nG}$	$n_B = -2.9$
$\lvert\mu\rvert < 5\times 10^{-8}$	$\Rightarrow$	$B_0 < 0.9\ \mathrm{nG}$	$n_B = -2.9$
PIXIE/COrE		$B_0 < 10^{-2}\ \mathrm{nG}$	$n_B = -2.2$

deep inside radiation dominated era $z_1 = 2\times 10^6$ $z_2 = 5\times 10^4$

$$\mu = -\frac{1.4}{3}(n_B+3)\left(\frac{\rho_{B,0}}{\rho_{\gamma,0}}\right)\left[\frac{1.08\times 10^{-2}\left(\frac{B_0}{\mathrm{nG}}\right)^{-1}}{k_c/\mathrm{Mpc}^{-1}}\right]^{n_B+3} \times \int_{z_1}^{z_2} dz\,(1+z)^{\frac{3n_B+7}{2}} e^{-\left(\frac{z}{z_{DC}}\right)^{\frac{5}{2}}}$$

assuming equipartition between magnetic modes: additional factor 2/3

KK, Komatsu ‘14

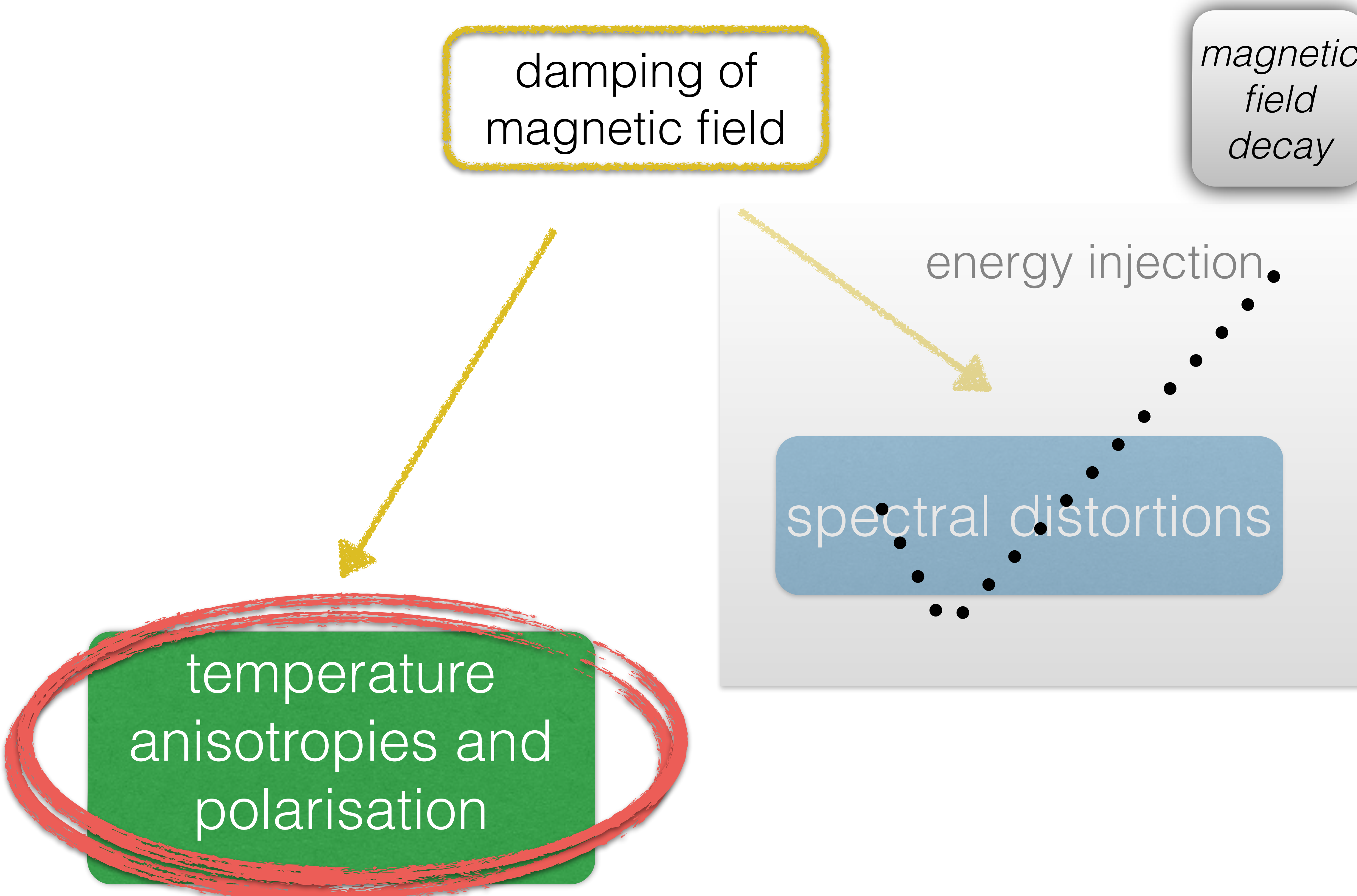
damping of
magnetic field
magnetic
field
decay
energy injection
spectral distortions
temperature
anisotropies and
polarisation

- Post-decoupling ionisation history changed by damping of magnetic fields

optical depth to Thomson scattering and visibility function modified.

Additional contribution to optical depth for $n_B < 0$

$$\Delta\tau(B_0, n_B) = 0.0241 \left(\frac{B_0}{\mathrm{nG}}\right)^{1.547} (-n_B)^{-0.0370} \times e^{-5.2815\times 10^{-12}(-n_B)^{23.8731} + 5.4\times 10^{-3}\left(\frac{B_0}{\mathrm{nG}}\right)^{3.3706} - 7.1\times 10^{-3}(-n_B)^{1.948}\left(\frac{B_0}{\mathrm{nG}}\right)^{2.0713}}$$

Planck13+WP

Maximal damping scale at decoupling:

$$k_{d,dec} = \frac{299.66}{\cos\theta}\left(\frac{B_0}{1\ \mathrm{nG}}\right)^{-1} \mathrm{Mpc}^{-1}$$

Effect of post-decoupling magnetic field damping on CMB anisotropies

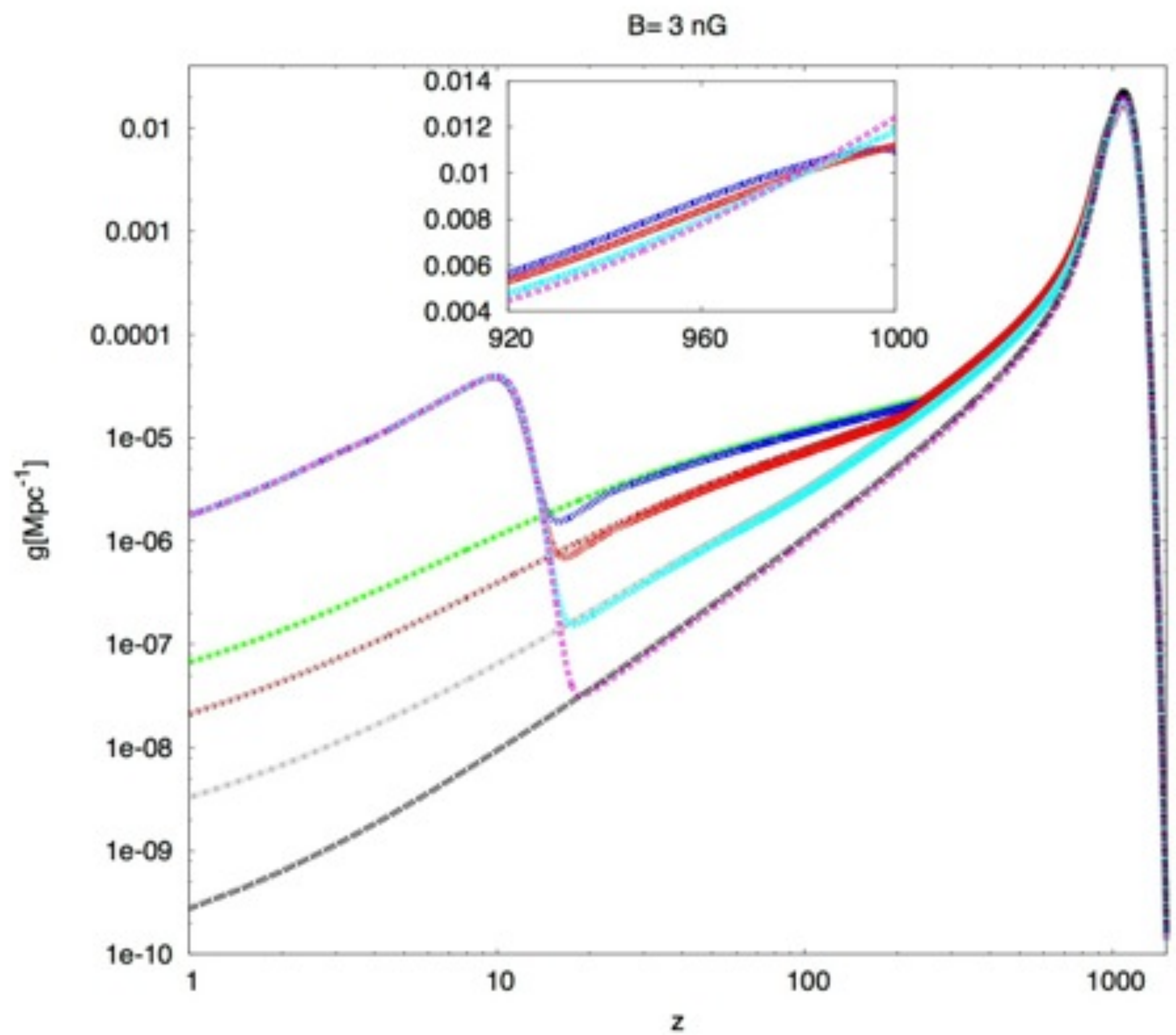

visibility function

$$g(z) \equiv \frac{d\tau}{dz} e^{-\tau(z)}$$

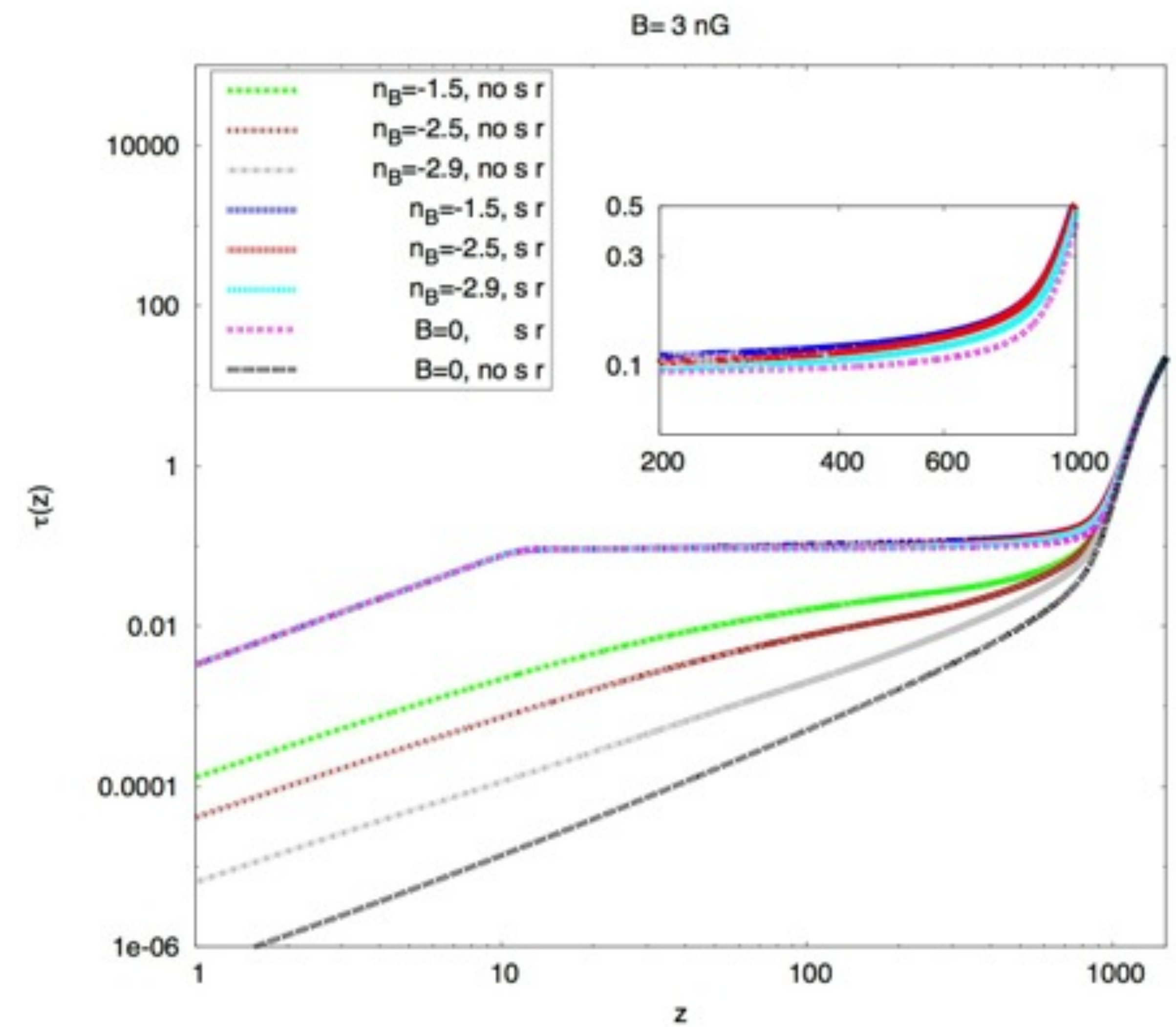

optical depth

$$\tau(z)_{B_0,n_B} = \int_0^z dz' \frac{\sigma_T c}{H(z')(1+z')} n_{e,B_0,n_B}(z')$$

KK, Komatsu ‘15

$$\tau_{tot} = \tau_{reio} + \tau_{high-z}$$

determined by
$\Delta\tau(B_0, n_B)$

C_ℓ^{EE}

at low ℓ not affected

magnetic field dissipation contributes

$$C_\ell^{TT} \to C_\ell^{TT} e^{-2\tau_{tot}}$$

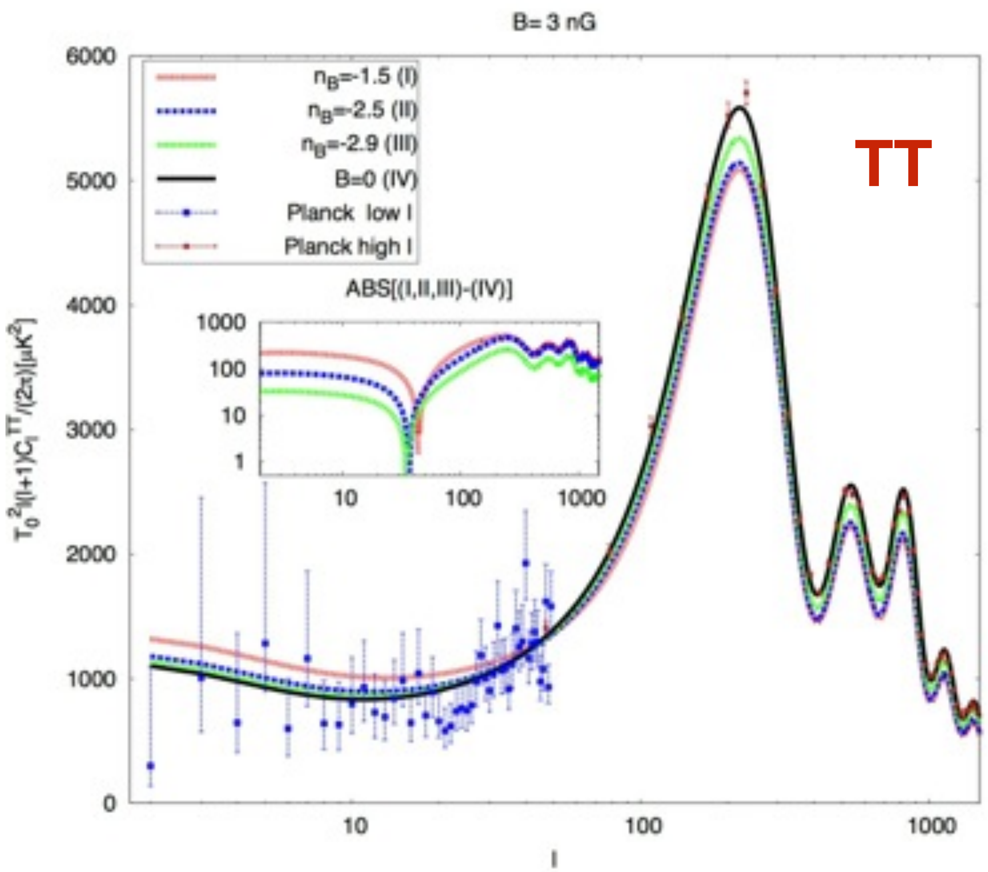

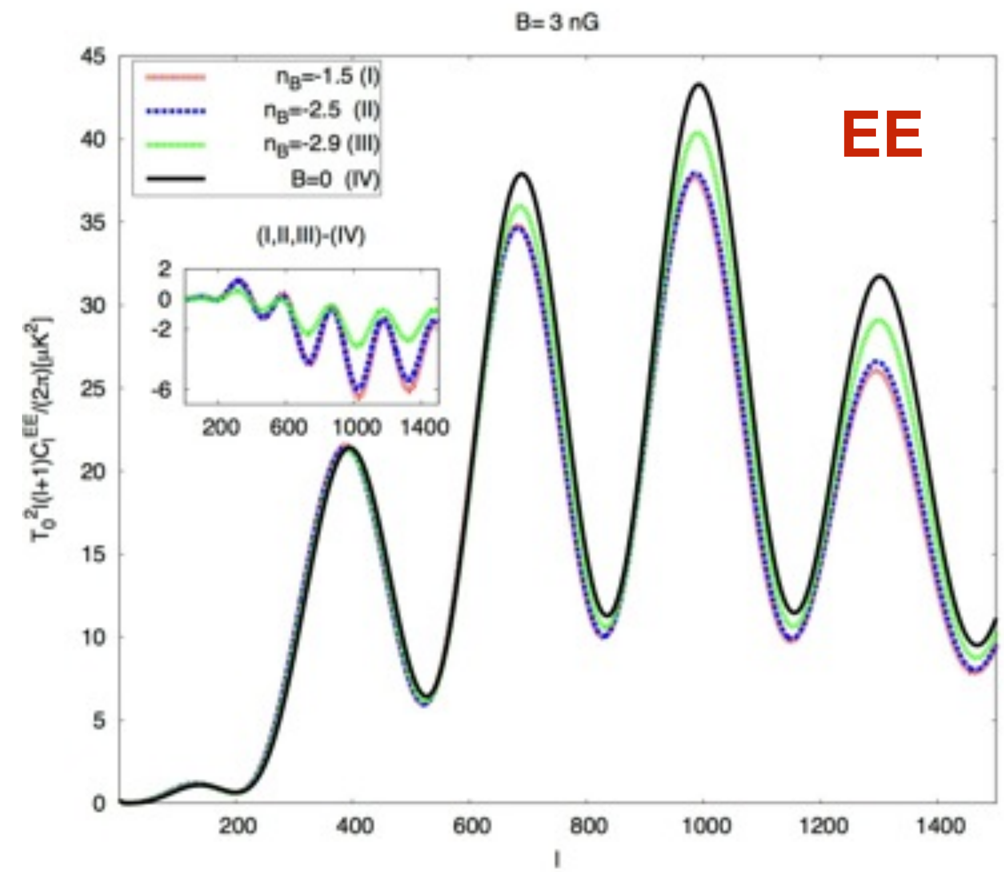

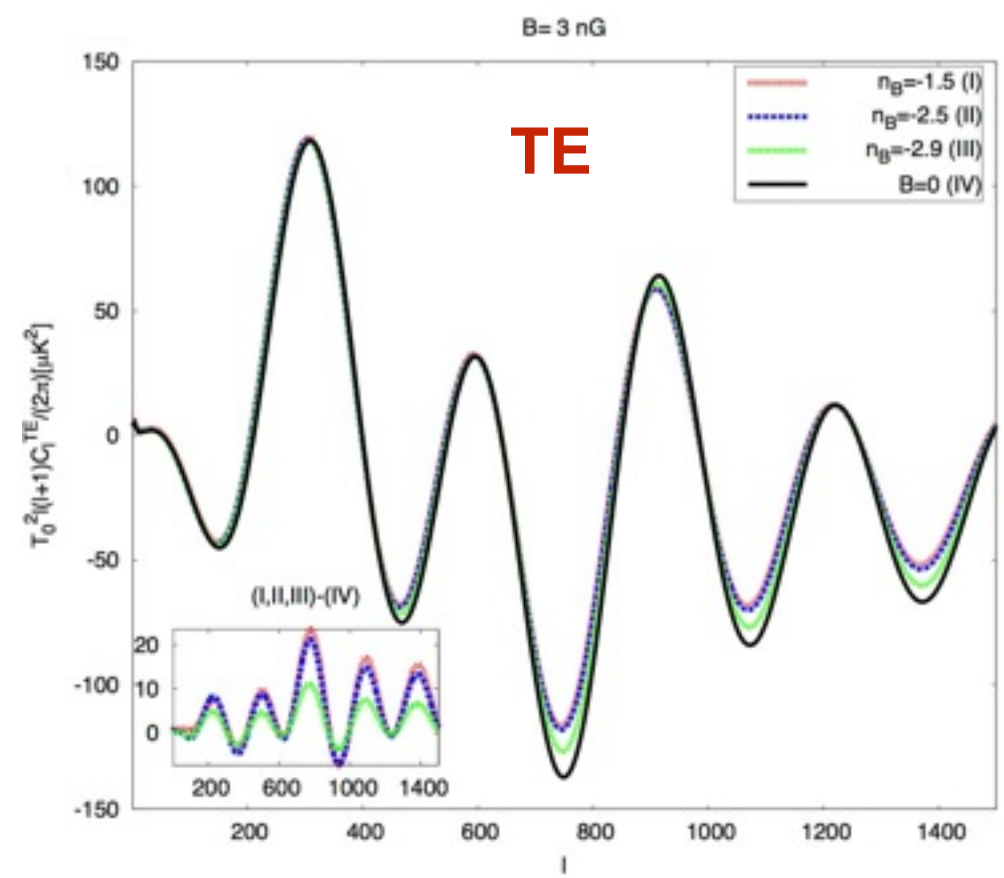

magnetic field parameters

$$B = 3\ \mathrm{nG}$$

$$n_B = -1.5,\ -2.5,\ -2.9$$

Planck13+WP

KK, Komatsu '15

Parameter estimation

2013 Planck data including the **CMB lensing data**, together with the likelihood of the **low-l polarization data from WMAP** as derived by the Planck collaboration

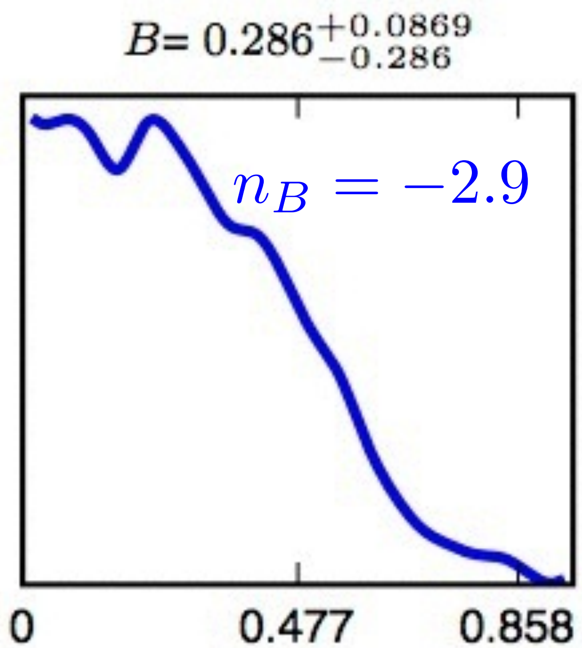

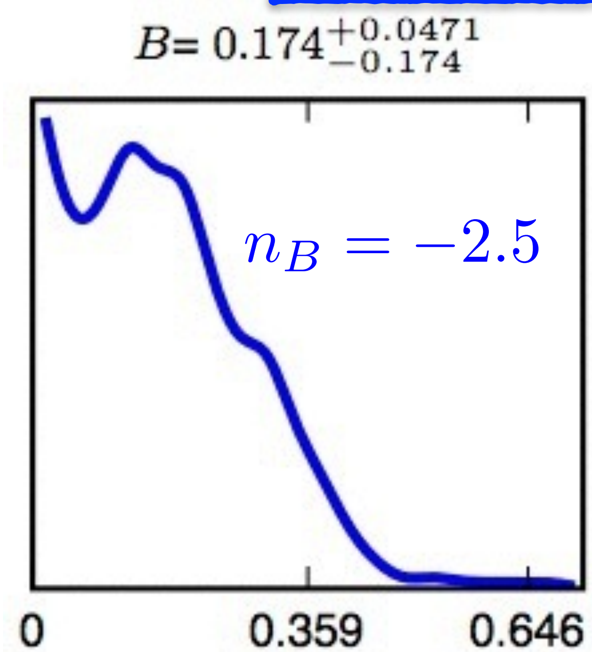

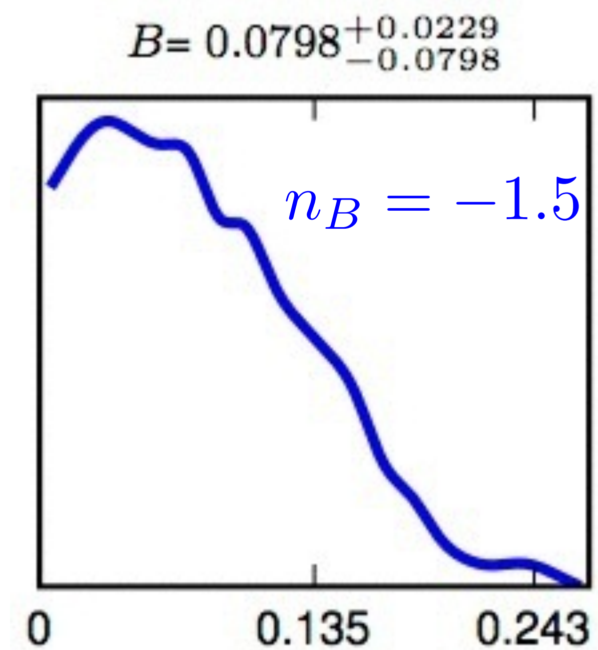

Marginalized posterior distributions of the magnetic field strength, B_0 (in units of nG)

	$n_B = -2.9$		$n_B = -2.5$		$n_B = -1.5$	
	best-fit	68% limits	best-fit	68% limits	best-fit	68% limits
B_0	0.2176	$0.286^{+0.087}_{-0.29}$	0.154	$0.1735^{+0.047}_{-0.17}$	0.06024	$0.07979^{+0.023}_{-0.08}$
$100\ \omega_b$	2.208	$2.214^{+0.027}_{-0.029}$	2.21	$2.215^{+0.027}_{-0.029}$	2.229	$2.214^{+0.028}_{-0.028}$
ω_{cdm}	0.12	$0.1188^{+0.0022}_{-0.0022}$	0.119	$0.1188^{+0.0022}_{-0.0022}$	0.1183	$0.1188^{+0.0022}_{-0.0022}$
H_0	67.22	$67.78^{+1}_{-1.1}$	67.66	$67.78^{+1}_{-1.1}$	68.14	67.74^{+1}_{-1}
$10^9 A_s$	2.172	$2.194^{+0.05}_{-0.053}$	2.225	$2.196^{+0.048}_{-0.056}$	2.188	$2.199^{+0.048}_{-0.056}$
n_s	0.9604	$0.9628^{+0.007}_{-0.0069}$	0.9663	$0.9626^{+0.0067}_{-0.007}$	0.9635	$0.9639^{+0.0074}_{-0.0075}$
τ_{reio}	0.08346	$0.08966^{+0.012}_{-0.014}$	0.09624	$0.09001^{+0.012}_{-0.014}$	0.08873	$0.08969^{+0.012}_{-0.014}$
$-\ln \mathcal{L}_{\min}$	4906.72		4906.63		4906.72	
$\chi^2_{\min}$	9813		9813		9813	

Table 1: Best-fit values and 68% confidence limits on the present-day magnetic field strength, B_0 (in units of nG), smoothed over $k_{d,dec}$ given in equation (1.1), and the standard ΛCDM cosmological parameters.

$$k_{d,dec} \simeq 299.66 \left(\frac{B_0}{1\ \mathrm{nG}}\right)^{-1} \mathrm{Mpc}^{-1}$$

modified version of CLASS + montepython

KK, Komatsu '15

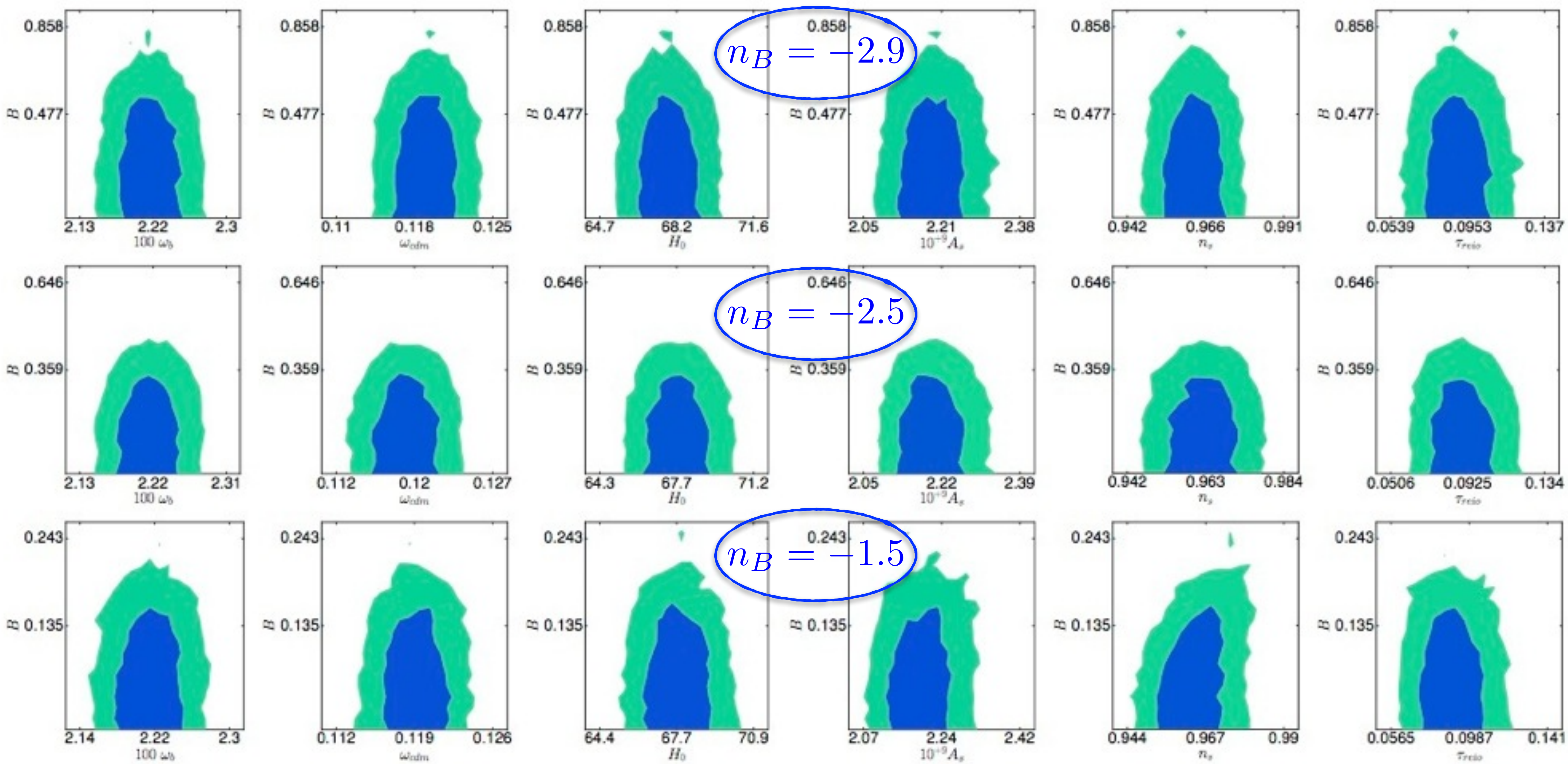

68% and 95% confidence regions of the field strength, B_0 (in units of nG), versus the cosmological parameters of the ΛCDM model

KK, Komatsu ‘15

The 95% CL upper bounds are $B_0 < 0.63$, 0.39, and 0.18 nG for $n_B = -2.9$, -2.5, and -1.5, respectively.

y distortion

$$y(n_B, B_0) = 1.2194 \times 10^{-5} \left(\frac{B_0}{\mathrm{nG}}\right)^{1.7263} (-n_B)^{0.3602}$$
$$-1.2155 \times 10^{-5} \left(\frac{B_0}{\mathrm{nG}}\right)^{1.7260} (-n_B)^{0.3619} \mathrm{e}^{9.3978\times 10^{-9}(-n_B)^{10.9842}}$$

$y < 10^{-9}$, 4×10^{-9}, and 10^{-9} for $n_B = -2.9$, -2.5, and -1.5, respectively

KK, Komatsu '15

Conclusions

- The *dissipation* of primordial magnetic fields opens up interesting possibilities to put strong limits on magnetic field parameters.